

CFD Simulation and Experimental Study of Winglets at Low Subsonic Flow

Sanjay Kumar Sardiwal¹, Md. Abdul Sami², B. V. Sai Anoop³, Syed Arshad Uddin⁴, Gudipudi Susmita⁵, Lahari Vooturi⁶,

^{1,2,3,5,6} Department of Aeronautical Engineering, MLR Institute of Technology, Hyderabad.

⁴ Departments of Aeronautical Engineering, Malla Reddy College of Engineering and Technology, Hyderabad

Abstract

A winglet is a device attached at the wingtip, used to improve aircraft efficiency by lowering the induced drag caused by wingtip vortices. It is a vertical or angled extension at the tips of each wing. Winglets work by increasing the effective aspect ratio of a wing without adding greatly to the structural stress and hence necessary weight of the wing structure. This paper describes a CFD 3-dimensional winglets analysis that was performed on a rectangular wing of NACA65₃218 cross sectional airfoil. The wing is of 660 mm span and 121 mm chord and was analyzed for two shape configurations, semicircle and elliptical. The objectives of the analysis were to compare the aerodynamic characteristics of the two winglet configurations and to investigate the performance of the two winglets shape simulated at selected cant angle of 0, 45 and 60 degrees. The computational simulation was carried out by FLUENT 6.2 solver using Finite Volume Approach. The simulation was done at low subsonic flow and at various angles of attack using Spalart-Allmaras couple implicit solver. A comparison of aerodynamics characteristics of lift coefficient C_L , drag coefficient C_D and lift to drag ratio, L/D was made and it was found that the addition of the elliptical and semi circular winglet gave a larger lift curve slope and higher Lift-to-Drag Ratio in comparison to the baseline wing alone. Elliptical winglet with 45 degree cant angle was the best overall design giving about 8 percent increase in lift curve slope and the best Lift-to-Drag Ratio.

Keywords— Aerodynamics, CFD, Elliptical winglet, Low subsonic, Semicircular winglet.

I. INTRODUCTION

A winglet is a device used to improve the efficiency of aircraft by lowering the lift induced drag caused by wingtip vortices [1]. It is a vertical or angled extension at the tips of each wing. Winglets improve efficiency by diffusing the shed wingtip vortex, which in turn reduces the drag due to lift and improves the wing's lift over drag ratio. Winglets increase the effective aspect ratio of a wing without adding greatly to the structural stress and hence necessary weight of its structure. Research into winglet technology for commercial aviation was pioneered by Richard Whitcomb in the mid 1970's. Small and nearly vertical fins were installed on a KC-135A and flights were tested in 1979 and 1980 [2]-[3]. Whitcomb revealed that in full size aircraft, winglets can provide improvements in efficiency of more than 7%. For airlines, this translates into millions of dollars in fuel costs.

Winglets are being incorporated into most new transport aircraft, including business jets, the Boeing 747-400, airliners, and military transport. The wingtip sail was the first industry application winglet studied by the Pennsylvania State University (PSU) [4]. 94-097 airfoil has been designed for use on winglets of high-performance sailplanes and tested in the Low-Speed, Low-Turbulence Wind Tunnel from Reynolds numbers of

0.24×10⁶ to 1.0×10⁶. Performance comparison was made between two well-known computer codes and experimental data, and both are found to generate results that are in good agreement with the wind tunnel measurements. Recent advancement in winglet was made in an Unmanned Aerial Vehicle (UAV) application where methods for designing and optimizing winglet geometry for UAVs were investigated at Reynolds numbers near 10⁶ [5]. The resulting methodology is then applied to existing UAV platforms for specific performance improvements.

The motivation for this research is to explore efficient shapes for winglet design. While research in winglets has been dominated by conventional winglets, with some research applied to multiple winglets [6], spiroid wingtip [7]-[8] and blended winglet [9]-[10], little is documented on the various shapes of elliptical and semicircular winglets. Lift and Drag analysis have been successfully studied experimentally, in an aircraft model using elliptical and semicircular winglets at 0 and 60 degree cant angle [11]-[12]. The main objective of this study is to numerically perform a CFD analysis on the baseline wings (without winglet) and winglets of semicircular and elliptical shapes at cant angle of 60 degree and an additional cant angle of 45 degree. The analysis were performed on rectangular wing of 660 mm span and

121 mm chord, at various angle of attack at low subsonic region (Mach number less than 0.3). The thickness of each winglet is half of the airfoil chord which is 60.5 mm. The study involved obtaining and comparing the aerodynamic characteristics such as drag coefficient, C_D , lift coefficient, C_L and lift-to-drag ratio, L/D .

II. METHODOLOGY

The computational steps in this project consist of three stages as shown in Figure 1. The project began from preprocessing stage of geometry setup and grid generation. The geometry of the model was drawn using CATIA V5R13. The grid was generated by GAMBIT. The second stage was computational simulation by FLUENT solver using Finite Volume Approach. Finally is the post-processing stage where the aerodynamics characteristics of the winglets were found.

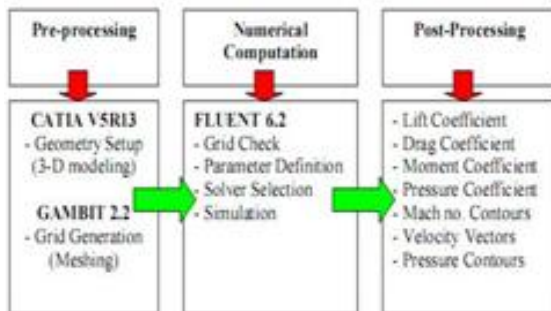


Fig. 1 The three stages of Project

Geometry setup was made using wireframe and surface design to draw the 3-dimensional model of winglet as shown in Figure 2. At the winglet wall and then incrementally increase up to the bullet shaped boundary wall. The sizing function scheme will help to reduce the number of element to be exported to FLUENT and also helps to reduce the computational time. The size function used was 10, 2, 10000 and it describes the start size, growth rate and size limit parameter respectively.

The numerical simulation by the solver was made after the completion of the mesh generation. The solver formulation, turbulence model Spalart-Allmaras, boundary condition, solution control parameters and material properties were defined. After all the parameters were specified, the model was initialized. The initializing and iteration processes stopped after the completion of the computations. The results obtained were examined and analyzed.

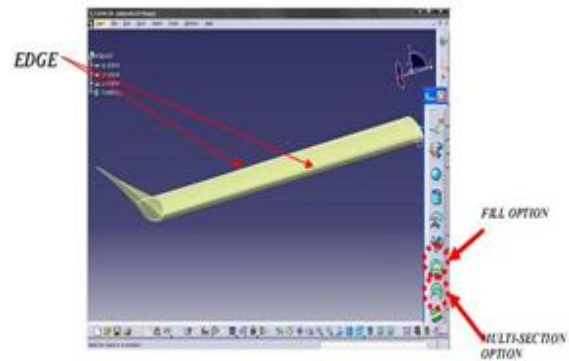


Fig. 2 Generated surface of wing and winglet

The 3-dimensional unstructured tetrahedral mesh was utilized for computing the flow around the model. Unstructured mesh is appropriate due to the complexity of the model. The advantages of the unstructured mesh are shorter time consumption in grid generation for complicated geometries and the potential to adapt the grid to improve the accuracy of the computation. After the meshing process, the mesh was examined. The purpose of examining the meshes was to check on the quality of the mesh by observing the skewness level and abrupt changes in cell sizes as shown in Figure 3.

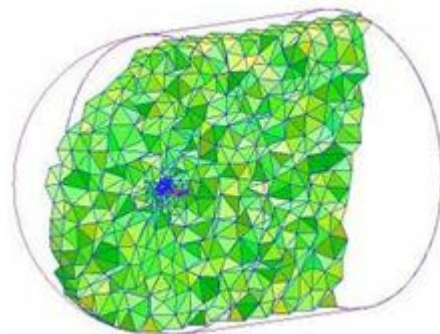


Fig. 3 Bullet shape computational domain and meshing examination

Then, the grids generated were developed using size function scheme in GAMBIT. This will enable finer mesh

III. RESULT AND DISCUSSION

The result from the 3-dimensional rectangular wing with winglet model was compared to the 3-dimensional rectangular wing without winglet. The discussions were focused on the aerodynamics characteristics which include drag coefficient C_D , lift coefficient C_L , and lift-to-drag ratio L/D . In addition, the pressure coefficient contours and pathlines will also be observed and studied. The simulation was carried out at various angles of attack, α , and Mach number less than 0.3. NACA airfoil section for rectangular wing was NACA65₂₁₈ airfoil and it stalled at 12 degree angle of attack. Thus, simulation

was done between 0 and 12 degree angles of attack at 40 m/s, 45 m/s and 50 m/s velocity respectively.

A) Lift Coefficient, C_L Analysis

Table 1 shows the lift coefficient C_L changes with angle of attack, α , for all winglet and rectangular wing models at velocity of 40, 45 and 50 m/s respectively.

Table 1. Lift Coefficient, C_L Comparison for different winglet configurations

Winglet Configuration	Velocity (m/s)	Lift Coefficient, C_L			
		0°	4°	8°	12°
Without Winglet	40	0.050573	0.30819	0.51212	0.67311
	45	0.050886	0.30873	0.51305	0.67435
	50	0.051128	0.30928	0.51393	0.67556
Elliptical Winglet (45° angle) Configuration1	40	0.077875	0.34352	0.57929	0.74795
	45	0.078123	0.34423	0.58045	0.7494
	50	0.07835	0.34491	0.58157	0.75077
Elliptical Winglet (60° angle) Configuration2	40	0.053246	0.30793	0.53289	0.68754
	45	0.053435	0.30853	0.53391	0.68878
	50	0.05359	0.30913	0.53489	0.68995
Semi Circular Winglet (45° angle) Configuration1	40	0.07701	0.33906	0.5724	0.74499
	45	0.077243	0.33971	0.57349	0.74638
	50	0.077451	0.34035	0.57455	0.74773
Semi Circular Winglet (60° angle) Configuration2	40	0.056687	0.30988	0.53092	0.68265
	45	0.056862	0.31049	0.53195	0.68394
	50	0.057047	0.31108	0.53298	0.68515

Figure 4 shows the elliptical winglet with cant angle of 45 degree has highest lift coefficient, C_L in comparison with other types of winglets. The semi circular winglet with cant angle of 45 degree gives the second highest lift coefficient, C_L . Both the elliptical and semi circular winglet with cant angle of 45 and 60 degree show an increase in the lift coefficient, C_L . Table 2 below shows the percentage increased in lift curve slope using winglet.

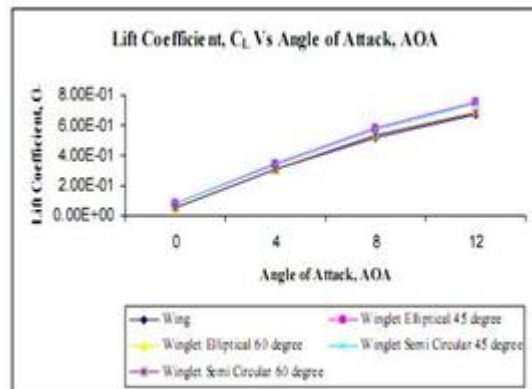


Fig. 4 Lift coefficient, C_L versus angle of attack, α , and velocity of 40 m/s

Table 2. Percentage increase in lift curve slope of different winglet types

Winglet Type	Lift Curve Slope Performance (% , percent)
Elliptical 45 degree	8.00
Elliptical 60 degree	2.82
Semi Circular 45 degree	6.97
Semi Circular 60 degree	1.43

B) Drag Coefficient, C_D Analysis

Table 3 shows the drag coefficient C_D changes with angle of attack, α for all winglet and rectangular wing models at velocity of 40, 45 and 50 m/s respectively.

Figure 5 shows drag coefficient, C_D versus angle of attack, α for all winglet and rectangular models at velocity of 40 m/s. From the graphs, the elliptical winglet with cant angle of 45 degree has the lowest drag coefficient, C_D followed by semi circular winglet of cant angle of 60 degree. All the elliptical and semi circular winglet with cant angle of 45 and 60 degree show a decrease in the drag coefficient, C_D .

Table 3. Drag Coefficient, C_D Comparison for different winglet configurations

Winglet Configuration	Velocity (m/s)	Drag Coefficient, C_D			
		0°	4°	8°	12°
Without Winglet	40	0.025739	0.036896	0.065364	0.11283
	45	0.025498	0.036385	0.065157	0.11272
	50	0.025312	0.036222	0.065017	0.11265
Elliptical Winglet (45° angle) Configuration1	40	0.025251	0.03595	0.061933	0.10255
	45	0.024982	0.035702	0.061762	0.10244
	50	0.024774	0.035517	0.06164	0.10238
Elliptical Winglet (60° angle) Configuration2	40	0.023913	0.033817	0.062604	0.10957
	45	0.023646	0.033564	0.062411	0.10946
	50	0.023437	0.033371	0.062268	0.10938
Semi Circular Winglet (45° angle) Configuration1	40	0.025758	0.036075	0.064492	0.11156
	45	0.025492	0.035826	0.064274	0.11144
	50	0.025285	0.035641	0.064125	0.11137
Semi Circular Winglet (60° angle) Configuration2	40	0.023935	0.033829	0.062338	0.10845
	45	0.023666	0.033579	0.062142	0.10834
	50	0.023458	0.033388	0.062001	0.10827

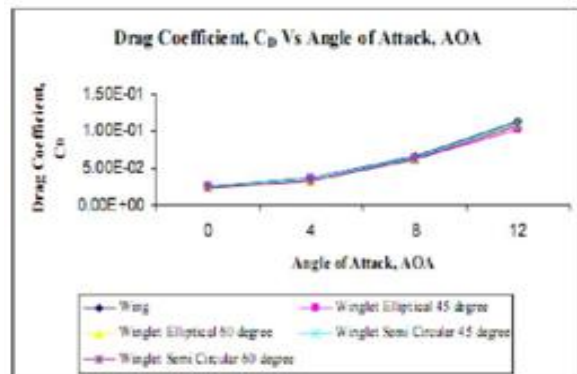


Fig. 5 Drag Coefficient, C_D at various angle attack, α and velocity of 40 m/s

C) Lift-To-Drag Ratio, C_L/C_D Analysis

Table 4 shows lift-to-drag ratio, C_L/C_D for all winglet and rectangular models at velocity of 40, 45 and 50 m/s respectively. Form the table 4 and figure 6 shown below, the elliptical winglet with cant angle of 45 degree has the highest lift-to-drag ratio, C_L/C_D compared to the other winglets for all velocities. This is followed by semi circular winglet with cant angle of 45 degree which is second highest lift- to-drag ratio, C_L/C_D for all velocities. All the elliptical and semi circular winglet with cant angle of 45 and 60 degree show the performance of increasing lift-to-drag ratio, C_L/C_D as shown in percentages in Table 5. It can also be seen that the most efficient angle of attack occur at 4 degree for this type of flow conditions.

Table 4. Comparison Lift-To-Drag Ratio, C_L/C_D for different winglet configurations

Winglet Configuration	Velocity (m/s)	Lift-to-Drag Ratio, C_L/C_D			
		0°	4°	8°	12°
Without Winglet	40	1.96	8.42	7.83	5.97
	45	2.00	8.49	7.87	5.98
	50	2.02	8.54	7.90	6.00
Elliptical Winglet (45° angle) Configuration1	40	3.08	9.56	9.35	7.29
	45	3.13	9.64	9.40	7.32
	50	3.16	9.71	9.43	7.33
Elliptical Winglet (60° angle) Configuration2	40	2.23	9.11	8.51	6.27
	45	2.26	9.19	8.55	6.29
	50	2.29	9.26	8.59	6.31
Semi Circular Winglet (45° angle) Configuration1	40	2.99	9.40	8.88	6.68
	45	3.03	9.48	8.92	6.70
	50	3.06	9.55	8.96	6.71
Semi Circular Winglet (60° angle) Configuration2	40	2.37	9.16	8.52	6.29
	45	2.40	9.25	8.56	6.31
	50	2.43	9.32	8.60	6.33

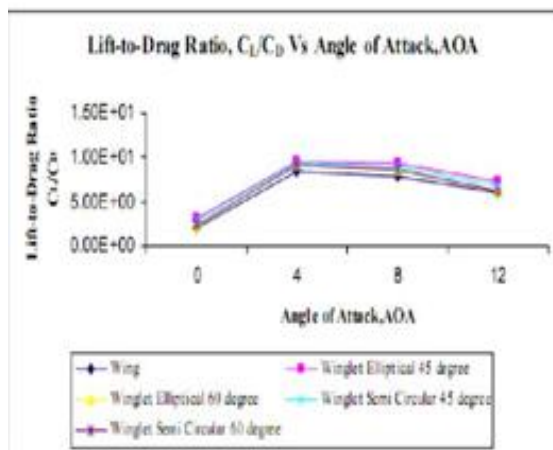


Fig.6 Lift-to-drag ratio, C_L/C_D at various angle attack, α and velocity of 40 m/s

Table 5 Percentage Increase of Different Winglet Types in Lift-To-Drag-Ratio, C_L/C_D over A Rectangular Wing

Winglet Type	Lift-to-Drag Ratio, C_L/C_D Performance (%. percent)
Elliptical 45 degree	17.62
Elliptical 60 degree	7.61
Semi Circular 45 degree	13.52
Semi Circular 60 degree	8.30

D) Pressure Coefficient Contours

Figure 7 until 10 below show pressure coefficient contour (top and bottom surface) of elliptical winglet at maximum velocity of 50 m/s and at 0 and 12 degree angle of attack. When the angle of attack, α increases, the upper surface will create a lower pressure coefficient. The high intensity blue area located on the upper surface suggests high lift is generated. At high angle of attack, α , lift is still capable of generating, but most of the total force is directed backward as drag.

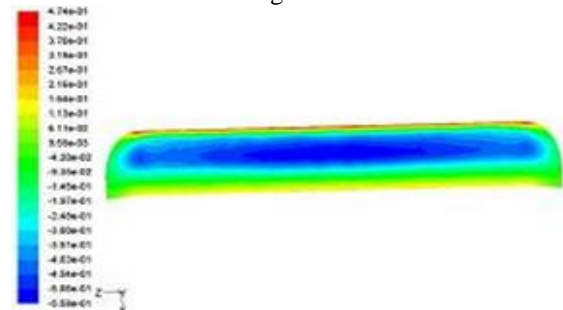


Fig. 7 Top C_p contours for elliptical winglet of 45 Degree Cant Angle at $\alpha = 0^\circ$

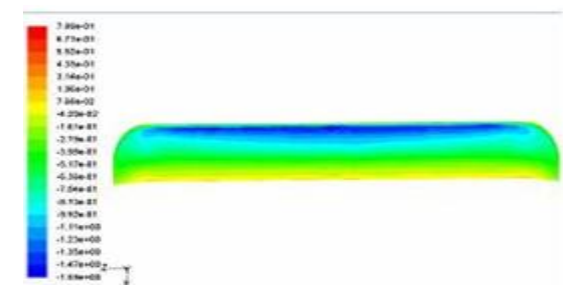


Fig. 8 Top C_p contours for elliptical winglet of 45 Degree Cant Angle at $\alpha = 12^\circ$

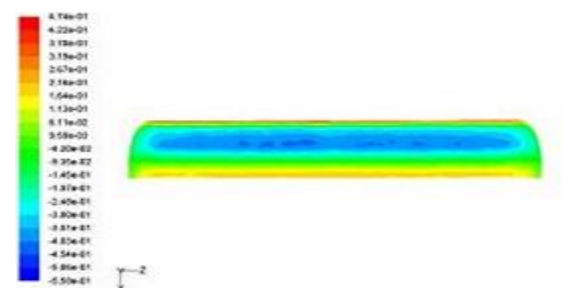


Fig. 9 Bottom C_p contours for elliptical winglet of 45 Degree Cant Angle at $\alpha = 0^\circ$

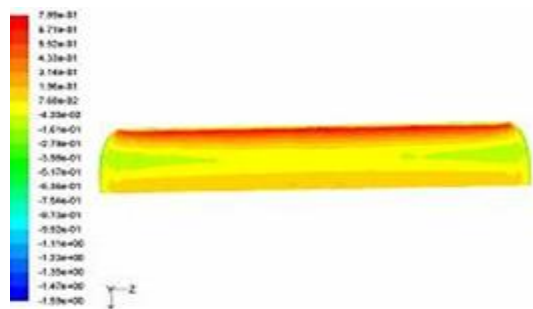


Fig. 10 Bottom C_p contours for elliptical winglet of 45 Degree Cant Angle at $\alpha = 12^\circ$

E) Pathlines

Figure 11 and 12 represent the pathlines view of flow over the studied winglets at maximum velocity of 50 m/s and maximum angle of attack of 12 degree. These pathlines are focused at the wingtip where trailing vortices occurs. The trailing vortices occur greatly at maximum angle of attack when an airplane takes off.

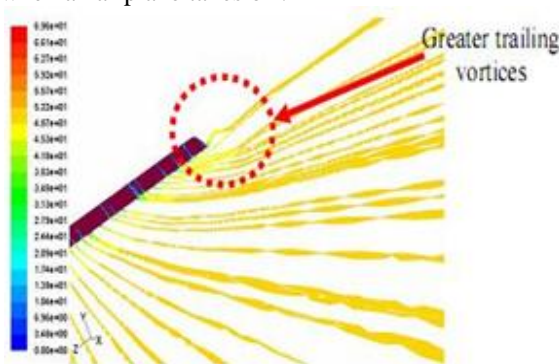


Fig. 11 Pathlines for Rectangular wing at $\alpha = 12^\circ$

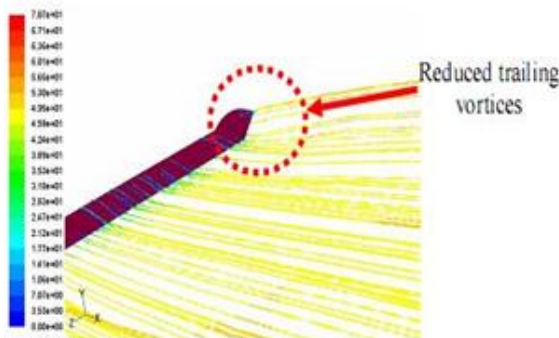


Fig. 12 Pathlines for Elliptical Winglet of 45 Degree Cant Angle at $\alpha = 12^\circ$

From the observation, the rectangular wing without winglet produces greater trailing vortices compare to the rectangular wing with winglet. The elliptical winglet with 45 degree cant angle greatly reduces the trailing vortices among all winglets.

IV. CONCLUSION

This project proposes alternatives in the design of winglet from the conventional designs. An

improved winglet design will significantly yield a better performance of an aircraft and reduce the fuel consumption. By using CFD to predict the performance of the winglets, huge amount of time and money can be saved before testing the winglet in the wind tunnel. Modification can also be done at this stage (during computational), thus shortening the time-cycle before actually coming out with the optimum design.

Despite the benefits of winglets, there are some drawbacks that need to be addressed. For example, the bending moment at the wing root is higher, and may require additional structural reinforcement of the wing. Winglets although can produce a low drag wing, they add to the cost and complexity of construction. They also modify the handling and stability characteristics. The viscous drag of the winglet can be too big, nullifying the reduction of the induced drag. Winglets have to be carefully designed so that these and other problems can be overcome.

REFERENCES

- [1] Yates, J. E., and Donaldson, C., "Fundamental Study of Drag and an Assessment of Conventional Drag-Due-To-Lift Reduction Devices", NASA Contract Rep 4004, 1986
- [2] Whitcomb, R. T., "A Design Approach and Selected Wind-Tunnel Results at High Subsonic Speeds for Wing-Tip Mounted Winglets", NASA N D-8260, 1976
- [3] Whitcomb, R. T., "Methods for Reducing Aerodynamic Drag", NASA Conference Publication 2211, Proceedings of Dryden Symposium, California 1981
- [4] Maughmer, M. D., Timothy, S. S., and Willits, S. M., "The Design and Testing of a Winglet Airfoil for Low-Speed Aircraft", AIAA Paper 2001-2478, 2001
- [5] J. Weierman and J. D. Jacob, "Winglet Design and Optimization for UAVs" 28th AIAA Applied Aerodynamics Conference, AIAA 2010-4224, 2010
- [6] S. Louis, B. G., "Spiroid-Tipped Wing", U. S. patent 5, 102,068., 1992
- [7] M.J Smith, N. Komerath, R. Ames, O. Wong, J. Pearson, "Performance analysis of a wing with multiple winglets" AIAA 19th Applied Aerodynamics Conference, Anaheim, CA, AIAA-2001-2407, 2001
- [8] A. Shelton, A. Tomar, J.V.R Prasad, M.J Smith et al. "Active multiple winglets for improved UAV performance" 22nd Applied Aerodynamics Conference and Exhibit, 16 - 19 August, Providence, Rhode Island AIAA 2004-4968, 2004
- [9] L.D Alford Jr, and G.J Clayman Jr ,

- “Blended Winglet” US Patent 7,644,892, 2010
- [10] R Grenon, and P Bourdin , “Numerical study of unconventional wing tip devices for lift-induced drag reduction” CEAS aerospace aerodynamics research conference, Cambridge (Grande Bretagne), June 10-13, 2002
- [11] Prithvi, R. A., Hossain, A., Jaafar, A. A., Edi, P., Younis, T. S., and Saleem, M., “Drag Reduction in Aircraft Model using Elliptical Winglet”, Journal of IEM, Malaysia, Vol. 66, No. 4. 2005
- [12] A Hossain, PR Arora, A Rahman, AA Jaafar, A , “Lift Analysis of an Aircraft Model with and without Winglet”, Proceedings of the International Conference on Mechanical Engineering 2007, 29- 31 December, Dhaka Bangladesh, 2007